Bioorganic & Medicinal Chemistry xxx (xxxx) xxx–xxx

Contents lists available at ScienceDirect

Bioorganic & Medicinal Chemistry

journal homepage: www.elsevier.com/locate/bmc

Chemical modification-mediated optimisation of bronchodilatory activity of mepenzolate, a muscarinic receptor antagonist with anti-inflammatory activity

Yasunobu Yamashita[a,1], Ken-ichiro Tanaka[b,1], Naoki Yamakawa[c,1], Teita Asano[d], Yuki Kanda[b], Ayaka Takafuji[b], Masahiro Kawahara[b], Mitsuko Takenaga[d], Yoshifumi Fukunishi[e], Tohru Mizushima[f,*]

[a] Technology Research Association for Next-Generation Natural Products Chemistry, 2-3-26 Aomi, Koto-ku, Tokyo 135-0064, Japan
[b] Department of Pharmaceutical Sciences, Musashino University, 1-1-20 Shinmachi, Nishi-Tokyo 202-8585, Japan
[c] Shujitsu University School of Pharmacy, 1-6-1, Nishigawara, Naka-ku, Okayama 703-8516, Japan
[d] Institute of Medical Science, St. Marianna University School of Medicine, 2-16-1, Sugao, Miyamae-ku, Kawasaki 216-8512, Japan
[e] Molecular Profiling Research Center for Drug Discovery (molprof), National Institute of Advanced Industrial Science and Technology (AIST), 2-3-26, Aomi, Koto-ku, Tokyo 135-0064, Japan
[f] LTT Bio-Pharma Co., Ltd, Shiodome Building 3F, 1-2-20 Kaigan, Minato-ku, Tokyo 105-0022, Japan

ARTICLE INFO

Keywords:
Chemical modification
Mepenzolate
COPD
Inflammatory
Long-acting muscarinic antagonist

ABSTRACT

The treatment for patients with chronic obstructive pulmonary disease (COPD) usually involves a combination of anti-inflammatory and bronchodilatory drugs. We recently found that mepenzolate bromide (**1**) and its derivative, 3-(2-hydroxy-2, 2-diphenylacetoxy)-1-(3-phenoxypropyl)-1-azoniabicyclo[2.2.2]octane bromide **(5)**, have both anti-inflammatory and bronchodilatory activities. We chemically modified **5** with a view to obtain derivatives with both anti-inflammatory and longer-lasting bronchodilatory activities. Among the synthesized compounds, (*R*)-(–)-**12** ((*R*)-3-(2-hydroxy-2,2-diphenylacetoxy)-1-(3-phenylpropyl)-1-azoniabicyclo[2.2.2]octane bromide) showed the highest affinity *in vitro* for the human muscarinic M3 receptor (hM_3R). Compared to **1** and **5**, (*R*)-(–)-**12** exhibited longer-lasting bronchodilatory activity and equivalent anti-inflammatory effect in mice. The long-term intratracheal administration of (*R*)-(–)-**12** suppressed porcine pancreatic elastase-induced pulmonary emphysema in mice, whereas the same procedure with a long-acting muscarinic antagonist used clinically (tiotropium bromide) did not. These results suggest that (*R*)-(–)-**12** might be therapeutically beneficial for use with COPD patients given the improved effects seen against both inflammatory pulmonary emphysema and airflow limitation in this animal model.

1. Introduction

Chronic obstructive pulmonary disease (COPD) is a serious health problem that is defined by a progressive and not fully reversible airflow limitation and an abnormal inflammatory response.[1–3] To treat COPD and to concomitantly elicit improved airflow by bronchodilation, it is important to suppress the inflammatory processes associated with this disease.

Both β2-agonists and muscarinic receptor antagonists are used clinically to achieve bronchodilation in the treatment of COPD.[2–4] Short-acting bronchodilators were previously used; however, in recent times long-acting -agonists (LABAs) and muscarinic receptor

Abbreviations: aclidinium, aclidinium bromide; BALF, bronchoalveolar lavage fluid; CDI, carbonyldiimidazole; COPD, chronic obstructive pulmonary disease; FEV0.1, forced expiratory volume in 0.1 s; FVC, forced vital capacity; glycopyrronium, glycopyrronium bromide; GST, glutathione S-transferase; hM_2R, human muscarinic M2 receptor; hM_3R, human muscarinic M3 receptor; HDAC2, Histone deacetylase 2; IFN, interferon; IL, interleukin; KC, keratinocyte chemoattractant; LABA, long-acting β2-agonist; LAMA, long-acting muscarinic antagonist; mepenzolate, mepenzolate bromide; MLI, mean linear intercept; [^{3}H]NMS, *N*-methyl-[^{3}H]-scopolamine methylchloride; PPE, porcine pancreatic elastase; QNB, 3-quinuclidinyl benzilate; ROS, reactive oxygen species; SOD, superoxide dismutase; tiotropium, tiotropium bromide; TNF, tumor necrosis factor

* Corresponding author.
E-mail address: t.mizushima@ltt.co.jp (T. Mizushima).
[1] These authors contributed equally to this work.

https://doi.org/10.1016/j.bmc.2019.06.016
Received 7 May 2019; Received in revised form 6 June 2019; Accepted 6 June 2019

antagonists (LAMAs) have replaced the shorter-acting ones due to their superior efficacy.[2,3] Tiotropium bromide (tiotropium), glycopyrronium bromide (glycopyrronium), and aclidinium bromide (aclidinium) are representative LAMAs used in the clinical setting.

The inflammation associated with COPD is typically treated with steroids; however, COPD disease progression is not fully suppressed by steroid treatment[4–6] because of resistance in part of the inflammatory processes to steroid treatment.[6,7] Histone deacetylase 2 (HDAC2) seems to play an important role in the inflammatory responses associated with COPD.[8–10] Because corticosteroids use HDAC2 to suppress inflammation,[8,11,12] the inhibitory effect of cigarette smoke on HDAC2 may be responsible for the reduced sensitivity of COPD patients to steroid treatment.[8] It is therefore important for new types of anti-inflammatory compounds to be developed to treat COPD.

From a library of medicines approved in Japan, we screened for compounds that suppress porcine pancreatic elastase (PPE)-induced pulmonary emphysema and inflammation in mice, and selected mepenzolate bromide (mepenzolate),[13] an orally administered muscarinic receptor antagonist used for the treatment of gastrointestinal disorders.[14–16] Mepenzolate exhibits not only anti-inflammatory effects via a muscarinic receptor-independent mechanism, but also provides short-acting bronchodilatory effects via a muscarinic receptor-dependent mechanism.[13,17,18] We previously reported that mepenzolate showed anti-inflammatory activity in PPE-induced pulmonary emphysema in mice.[13] We also showed that steroids and other anti-inflammatory drugs did not demonstrate anti-inflammatory activity in the same PPE models,[19] suggesting that the anti-inflammatory activity of mepenzolate is more potent than that of steroids. The anti-inflammatory activity of mepenzolate is mediated via a decreased level of reactive oxygen species (ROS) in the lung due to the NADPH oxidase activity and the induction of superoxide dismutase (SOD) and glutathione S-transferase (GST) expression.[13]

We previously postulated that mepenzolate derivatives possessing both anti-inflammatory and long-acting bronchodilatory activities might be beneficial for the treatment of COPD. To obtain such derivatives, we synthesized hybrid compounds based on mepenzolate and glycopyrronium or aclidinium, and found that one of these hybrid compounds (3-(2-hydroxy-2, 2-diphenylacetoxy)-1-(3-phenoxypropyl)-1-azoniabicyclo[2.2.2]octane bromide **(5)** showed both a longer-acting bronchodilatory activity (equivalent to glycopyrronium and aclidinium) and possessed anti-inflammatory properties (equivalent to mepenzolate).[20] Based on these results, in the present study we chemically modified **5** to obtain derivative compounds with both anti-inflammatory and even longer-acting bronchodilatory activities. As for synthesized hybrid compounds based on mepenzolate bromide (**MP**), glycopyrronium bromide (**GC**), and aclidinium bromide (**AD**), both **MP-GC** and **MP-AD** showed anti-inflammatory effects similar to **MP**, whereas **GC-MP**, like **GC** and **AD** alone, did not.[20] Based on these results, we speculated here that the double phenyl rings in **MP** (Fig. 1) are important for its anti-inflammatory activity and therefore, we avoided modifying this part. Instead, we chemically modified the terminal phenyl ring combined with the nitrogen atom of quinuclidine. Among the derivatives obtained, (*R*)-(–)-**12** showed the highest affinity for hM_3R *in vitro* and the longest bronchodilatory activity *in vivo*, with an anti-inflammatory effect similar to that of **5** and mepenzolate. These results suggest that (*R*)-(–)-**12** might be therapeutically beneficial in a clinical setting for COPD patients.

2. Results

2.1. Chemistry

The route followed to synthesize target compounds **6–14** and **15–27** is outlined in Scheme 1. QNB (3-quinuclidinyl benzilate) (**28**) was the key compound used for synthesizing all target compounds. Subsequent quaternization of **28** with an appropriate alkyl bromide (**29–50**) in 1,4-dioxane provided the desired corresponding target compounds **6–27**. The enantiomers (*R*)-(–)-**12** and (*S*)-(+)-**12** were synthesized in the same manner as that for (*R*)-(–)-**1** and (*S*)-(+)-**1** with enantiomerically pure 3-quinuclidinol instead of racemic 3-quinuclidinol.[21] All of the new target compounds were characterized by NMR and HRMS. Protocols for the synthesis and characterization of final compounds **6–27** and intermediates **29–50** are described in the supporting information.

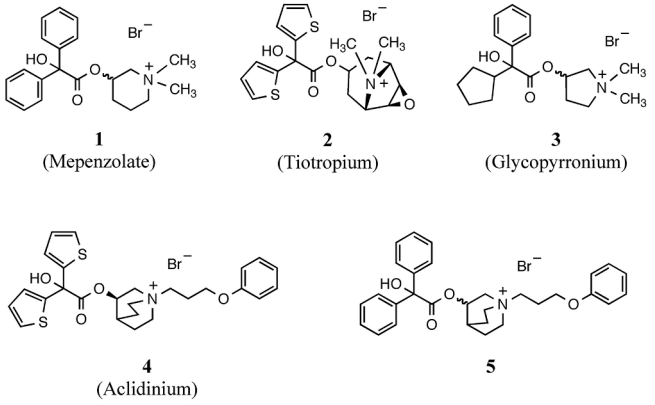

Fig. 1. Structure of clinically-used muscarinic antagonists **1–4** and hybrid compound **5**.

2.2. Chemical modifications to mepenzolate

The binding affinity of each compound to hM_3R was determined by carrying out *N*-methyl-[^{3}H]-scopolamine methylchloride ([^{3}H]NMS) displacement studies on this receptor. The binding affinities of mepenzolate (**1**), tiotropium (**2**), glycopyrronium (**3**), aclidinium (**4**) and compound **5** (Fig. 1) are shown in Table 1 (data for **1–5** are from our previous report[20]). The affinity of **5** for hM_3R was higher than that of **1** but lower than that of **2**.[20]

The total number of leucocytes and the individual number of neutrophils in bronchoalveolar lavage fluid (BALF) are indicators of pulmonary inflammatory responses; we previously showed that increases in these numbers after PPE treatment were partially suppressed by the simultaneous intratracheal administration of **1** and **5**.[13,17,20] On the other hand, none of **2–4** showed anti-inflammatory activity.[20] Based on these findings, we attempted to identify derivatives of **5** that have an affinity for hM_3R similar to that of **2** and an anti-inflammatory activity similar to that of **1** and **5**. Because the high affinities of drugs for hM_2R are associated with adverse effects on cardiac function,[22] compounds that showed a higher affinity for hM_3R than for hM_2R were preferred and thus the focus of the selection process used in this study.

The strategy used for making chemical modifications to **5** is shown in Fig. 2. We modified the linker moiety of **5** (Scheme 1), first shortening (**6** and **7**) or extending (**8** and **9**) the linker length of **5**. We also changed the linker moiety of **5** into a carbon chain without a heteroatom (**10–14**), with **12** found to have the highest affinity for hM_3R (Table 1). As for hM_2R, **12** showed a slightly lower affinity (Table 1).

A variety of substituents were then introduced into the terminal phenyl ring combined with the linker of **12** to obtain derivatives thereof (**15–27**) (Scheme 1). However, the simplest analogue **12**, which had no substituent on the terminal phenyl ring, showed the highest affinity for hM_3R. Based on these results, **12** was selected for further analysis.

2.3. Synthesis and activity of enantiomers of mepenzolate derivatives

As for **1**, **12** has one asymmetric carbon atom, enabling it to exist in two enantiomeric forms (Fig. 2), for which a racemic mixture of these two enantiomers was used in the experiments described above. We recently reported that although anti-inflammatory activity was

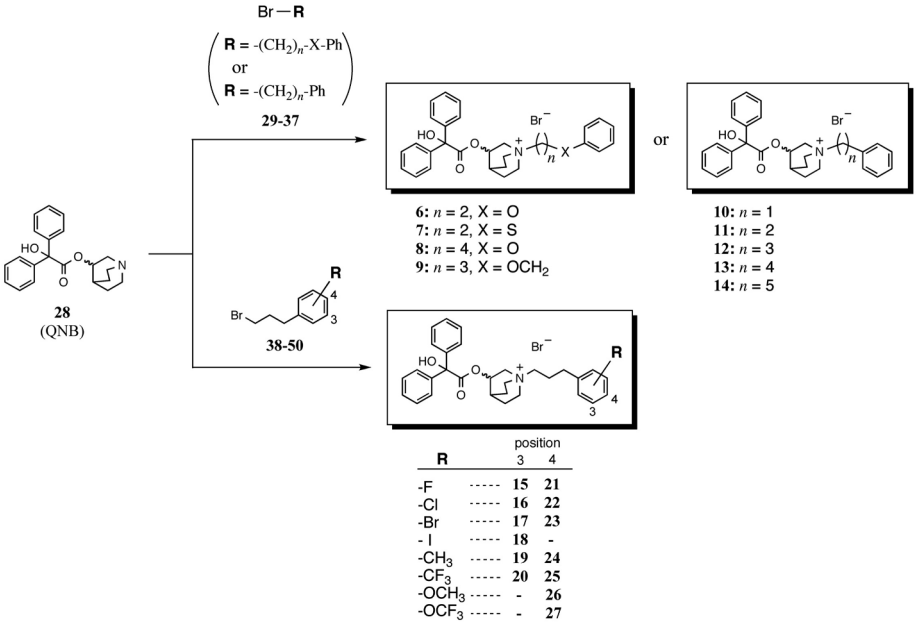

Scheme 1.

indistinguishable between enantiomers (*R*)- (–)-mepenzolate (*R*)-(–)-**1** and (*S*)-mepenzolate (*S*)-(+)-**1**, the binding affinity of (*R*)-(–)-**1** to hM_3R *in vitro* and its bronchodilatory activity *in vivo* were superior to that of (*S*)-(+)-**1**[21].

We have synthesized (*R*)-(–)-**12** and (*S*)-(+)-**12**, and examined their biochemical and pharmacological activities. As shown in Table 1, (*R*)-(–)-**12** exhibited a higher affinity for hM_3R than (*S*)-(+)-**12**. We also compared their bronchodilatory activities. As shown in Fig. 3A, at a dose of 48 μg/kg, **12** and (*R*)-(–)-**12** but not (*S*)-(+)-**12** showed bronchodilatory activity. These *in vivo* results were consistent with the *in vitro* results for hM_3R affinity (Table 1). On the other hand, the measured anti-inflammatory activity was indistinguishable among **12** and its enantiomers ((*R*)-(–)-**12** and (*S*)-(+)-**12**) (Fig. 4A). Taken together, these results suggest that (*R*)-(–)-**12** may be preferable to (*S*)-(+)-**12**, and that the higher affinity for hM_3R of the (*R*)-enantiomer compared with the (*S*)-enantiomer was a general property of mepenzolate derivatives.

2.4. Bronchodilatory and anti-inflammatory activities of R-12

We next compared the bronchodilatory activities of **1**–**5** and (*R*)-(–)-**12**, beginning with their dose–response profiles. A dose of 38 μg/kg for **1** corresponds to 42, 36, 50, 49 and 48 μg/kg for **2**, **3**, **4**, **5**, and (*R*)-(–)-**12**, respectively, based on their molecular weights. As shown in Fig. 3B, 1 h after administration of each drug, complete suppression of the methacholine-induced increase in airway resistance was observed with **2** and (*R*)-(–)-**12** at doses of 4.2 and 4.8 μg/kg, respectively. We recently reported that complete suppression of the methacholine-induced increase in airway resistance was observed with **1**, **3**, **4**, and **5** at doses of 38, 3.6, 5.0 and 4.9, respectively.[20] These results suggest that (*R*)-(–)-**12** has a strong bronchodilatory activity, similar to that of **2** which is currently used in the clinical setting.

We subsequently compared the duration of bronchodilatory activity exhibited by the derivative compounds. We previously found that the bronchodilatory activity of **1** disappeared within 24 h of its administration.[20] We also showed that the bronchodilatory activities of **3** and **4** (clinically used LAMAs) were still present 48 h after their administration, but had disappeared by 72 h.[20] As shown in Fig. 5A, bronchodilatory activity with **3**, **4**, and **5** was not observed up to 96 h after drug administration. On the other hand, (*R*)-(–)-**12** and **2** still showed bronchodilatory activity at 96 or 120 h, respectively, after administration (Fig. 5A, B), suggesting that (*R*)-(–)-**12** exhibits long-acting bronchodilatory activity, similar to that of **2**.

An examination of anti-inflammatory activity revealed that **1** and (*R*)-(–)-**12** significantly suppressed the PPE-induced increase in the total number of leucocytes and the individual number of neutrophils in BALF (Fig. 4B). We recently reported a similar anti-inflammatory effect for **5**, but not for **2**-**4**.[20]

We next examined the mechanism underlying (*R*)-(–)-**12**'s anti-inflammatory activity. As shown in Fig. 4C, PPE-induced an increase in the mRNA expression of tumor necrosis factor (*TNF)-α*, interleukin (*IL-6)*, interferon (*IFN)*-γ, and keratinocyte chemoattractant (*KC)*; this expression was suppressed by the administration of (*R*)-(–)-**12** in all cases. Furthermore, administration of (*R*)-(–)-**12** to healthy mice increased GST activity in the lung, suggesting that this effect is involved in the anti-inflammatory activity of (*R*)-(–)-**12**, as in the case of **1**.[13]

2.5. Effect of 2 and R-12 on PPE-induced lung injury and dysfunction

The effects of the long-term administration of **2** and (*R*)-(–)-**12** on lung injury and dysfunction induced by PPE were compared. Histopathological analysis revealed that PPE induced damage to the alveolar walls and an increase in the mean linear intercept (MLI; an indicator of airspace enlargement). These effects could be partly suppressed by the administration of (*R*)-(–)-**12** but not by **2** (Fig. 6A and B).

PPE-induced lung dysfunction can be monitored by using the $FEV_{0.1}/FVC$[19,23]. While the PPE treatment decreased the $FEV_{0.1}/FVC$ ratio, administration of (*R*)-(–)-**12** but not **2** significantly restored the towards control values (Fig. 6C). The results presented in Fig. 6 suggest that the long-term administration of (*R*)-(–)-**12**, but not of **2**, suppress PPE-induced lung injury and dysfunction.

3. Discussion

We have chemically modified **5** to produce derivatives with both anti-inflammatory and longer-lasting bronchodilatory activities. Although a drug's affinity for hM_3R is not always correlated with its duration of action, we selected this index for the initial screening of drugs given that hM_3R affinity can be rapidly determined for large panels of compounds. Of all the derivatives synthesized, **12** showed the highest affinity for hM_3R. Compound **12** has an asymmetric carbon atom, with (*R*)-(–)-**12** exhibiting a higher affinity for hM_3R *in vitro* and

Table 1
Binding of compounds to hM2R or hM3R. Membrane fractions prepared from CHO-K1 cells expressing hM2R or hM3R were incubated with 2 nM [^{3}H]NMS (85.5 Ci/mmol) in the presence of each compound. A range of concentrations (10^{-11} to 10^{-6} M) for each compound was tested to generate competition curves to determine K_i values. At the initial screening, we examined affinity values from triplicate measurements and determined mean values. For some compounds that showed a relatively high affinity at the initial screening, we re-examined the affinity in independent experiments and confirmed the results. Mean values of triplicate data for each one experiments are shown in the table. Compounds whose affinity values were re-examined in additional experiments are denoted by an asterisk (*). Data for **1**–**5** are from our previous report [20]. Values represent mean ± S.E.M.

Compound	K_i (nM)	
	hM_3R	hM_2R
1	5.3 ± 2*	2.1 ± 2*
2	0.20 ± 0.02*	0.49 ± 0.2*
3	0.81 ± 0.2*	1.6 ± 0.7*
4	0.56 ± 0.3*	0.43 ± 0.04*
5	0.88 ± 0.1*	0.68 ± 0.1*
6	2.8 ± 0.08	—
7	0.65 ± 0.4*	0.40 ± 0.2*
8	41 ± 21	12 ± 0.2
9	42 ± 12	12 ± 1
10	81 ± 39	21 ± 3*
11	0.86 ± 0.4	2.3 ± 0.2*
12	0.44 ± 0.04*	0.72 ± 0.01
13	4.7 ± 0.6*	12 ± 0.5
14	17 ± 0.4	7.1 ± 2
15	1.1 ± 0.3	0.69 ± 0.04
16	6.5 ± 2	2.1 ± 1*
17	20 ± 16	9.2 ± 2
18	3.8 ± 2	—
19	1.9 ± 0.6	1.4 ± 0.5
20	19 ± 4	—
21	1.7 ± 0.2	0.49 ± 0.2
22	0.51 ± 0.1*	0.11 ± 0.1
23	2.6 ± 0.4	1.6 ± 0.3
24	0.86 ± 0.4*	1.1 ± 0.5
25	2.3 ± 2	0.18 ± 0.1
26	7.8 ± 2	0.91 ± 0.7
27	1.5 ± 0.1	2.6 ± 0.3
(*R*)-(–)-12	0.40 ± 0.06*	1.0 ± 0.2*
(*S*)-(+)-12	184 ± 30*	68 ± 28*

—, not tested.
* , more than two independent experiments were performed.

longer bronchodilatory activity *in vivo* than (*S*)-(+)-**12**. Compound (*R*)-(–)-**12** was thus selected for further study of its pharmacological activities compared to those of clinically used LAMAs.

The results in this study suggest that the length of the linker moiety (between the nitrogen atom of quinuclidine and the terminal phenyl ring) is an important parameter determining a compound's affinity for hM_3R, and that chemical modification of the terminal phenyl ring is not an effective measure to increase affinity for hM_3R. It was reported that the mode of interaction of **2** with the muscarinic receptors is unique,[24] with the results in this study suggesting that (*R*)-(–)-**12** has a similar interaction mode to that of tiotropium. Further study is needed to examine the nature of (*R*)-(–)-**12**'s mode of interaction with hM_3R. In addition, investigation of interaction of (*R*)-(–)-**12** with the other muscarinic receptor subtypes is also important in order to understand the molecular mechanism of its pharmacological action.

Previously, we examined the effect of intratracheal administration of **2** on increased fecal pellet output induced by restraint stress. As a result, compared to the protective effect of **2** against PPE-induced lung injury, more than 100 times higher dose of **2** was required to affect fecal pellet output.[17] We assumed that this is due to the low efficiency of intratracheally administered **2** to transfer to blood, because we showed that the blood concentration of **2**, 1 min after the intratracheal administration (10 mg) was 3 μg/ml, whereas that of intravenous administration (7.5 mg) was 40 μg/ml.[17] Based on these results, we speculate that intratracheally administered (*R*)-(–)-**12** also has less effect on organs (such as colon) other than lung and bronchi, compared to its respiratory effects.

Comparison of the activities of (*R*)-(–)-**12** and of clinically used LAMAs (**2–4**) revealed that the duration of bronchodilation by (*R*)-(–)-**12** was longer than that of **3**–**5** and similar to that of **2**. The long-term intratracheal administration of (*R*)-(–)-**12**, but not of **2**, also suppressed PPE-induced pulmonary emphysema and respiratory dysfunction. These results suggest that (*R*)-(–)-**12** might be therapeutically beneficial for the treatment of COPD patients given that (*R*)-(–)-**12** appears to have beneficial effects against both inflammation-induced pulmonary emphysema and airflow limitation. While we selected the elastase model for the initial evaluation of candidate drugs given the rapid and acute effects seen therein, further studies with other models, such as the cigarette smoke model,[25] would be important to further characterize the properties of candidate drugs. Patent applications have been submitted for (*R*)-(–)-**12** and related compounds.

4. Materials and methods

More detailed descriptions concerning the methods are provided in the Supplementary Information.

4.1. Synthesis of targeted compounds and purity analyses.

Methods for the synthesis of targeted compounds are described in the Supplementary Information. HPLC analysis was used for determining the purity of targeted compounds, with a purity of greater than 95% purity confirmed for all cases.

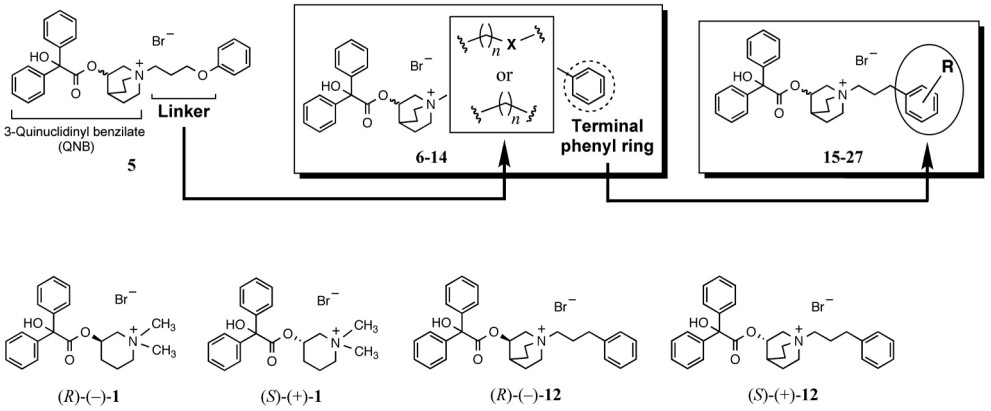

Fig. 2. Strategy used for making chemical modifications to **5** and structures of enantiomers of **1** ((*R*)-(–)-**1** and (*S*)-(+)-**1**) and **12** ((*R*)-(–)-**12** and (*S*)-(+)-**12**)..

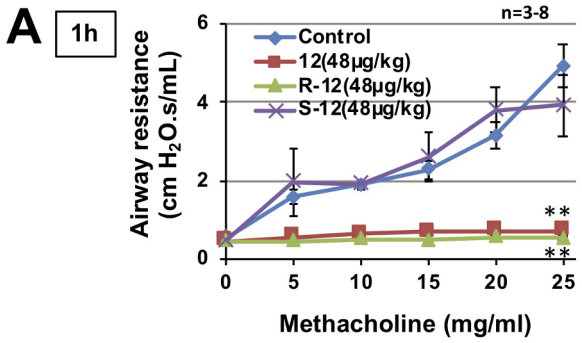

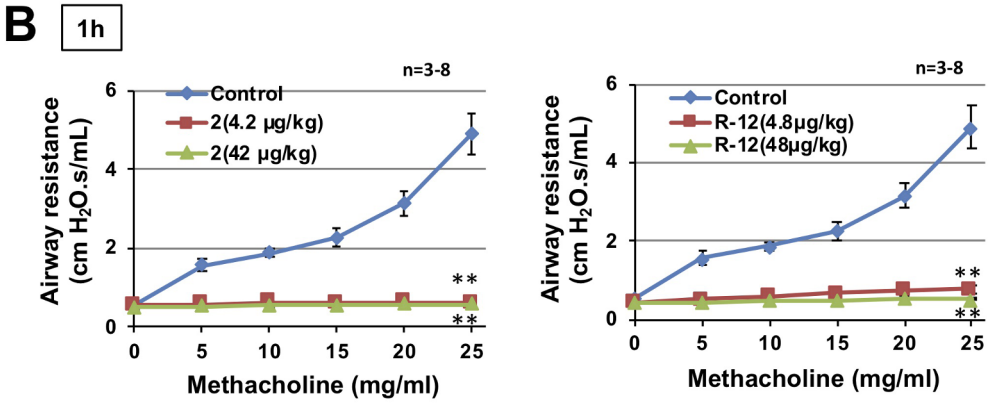

Fig. 3. Dose-response curves for compounds **12**, (*R*)-(–)-**12**, and (*S*)-(+)-**12** (A) or **2** and (*R*)-(–)-**12** (B) for methacholine-induced airway constriction. Indicated doses were administered intratracheally. After 1 h, mice were exposed to nebulized methacholine five times and airway resistance was determined after each methacholine challenge as described in the Materials and Methods. Values represent mean ± S.E.M. $^{*}P < 0.05$. Control data are the same in all graphs. Data are representative of two independent experiments.

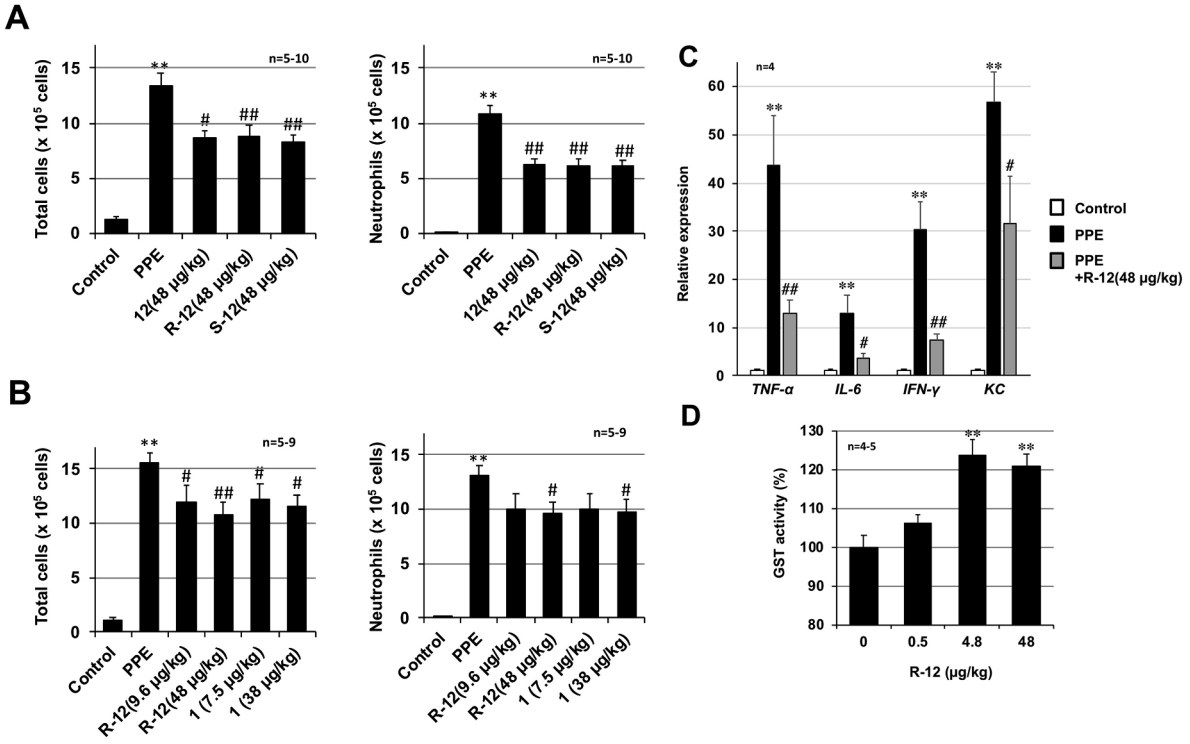

Fig. 4. Effect of compounds on PPE-induced inflammatory responses. Mice were treated with or without (control) PPE (20 U/kg) once only on day 0 (A, B, C). The indicated doses (μg/kg) of compounds were administered intratracheally once only (A, B, C). Twenty-four hours after the PPE administration, BALF was prepared and the total cell number and the number of neutrophils were determined as described in the Materials and Methods (A, B). Twenty-four hours after the PPE administration, total RNA was extracted from lung tissue and subjected to real-time RT-PCR using a specific primer set for each gene. Values were normalized to *Hprt1* and expressed relative to the Control (C). Male ICR mice were administered intratracheally with indicated doses (μg/kg) of (*R*)-(–)-**12** or vehicle (saline) once only. Twenty-four hours after the (*R*)-(–)-**12** administration, lung homogenates were prepared. GST activity was determined as described in the Materials and Methods (D). Values represent mean ± S.E.M. $^{**}P < 0.01$ (versus control); $^{\#}P < 0.05$, $^{\#\#}P < 0.01$ (versus PPE only); n.s., not significant. Data are representative of two independent experiments.

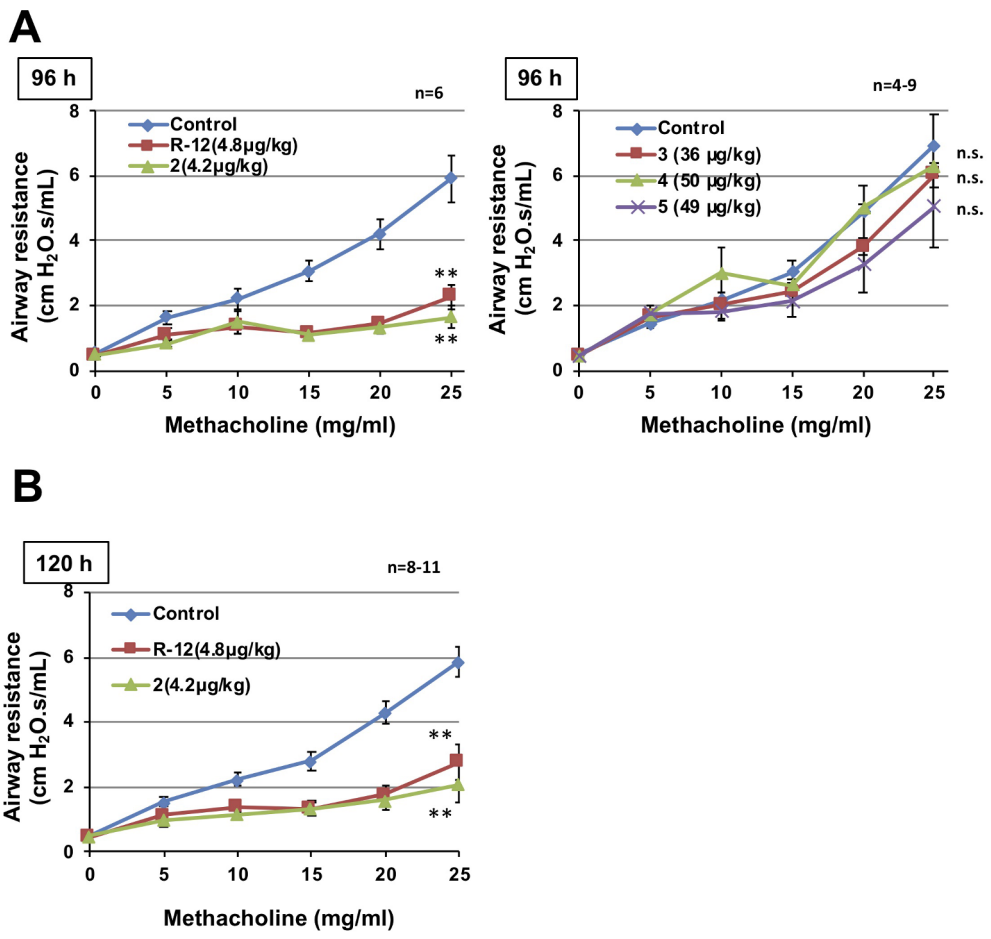

Fig. 5. Time-course of effect of compounds **2**, **3**, **4**, **5** and (*R*)-(–)-**12** (A) or **2** and (*R*)-(–)-**12** (B) on methacholine-induced airway constriction. Indicated doses were administered intratracheally. After 96 h (A) or 120 h (B), mice were exposed to five cycles of nebulized methacholine and airway resistance was determined after each methacholine challenge as described in the Materials and Methods. Values represent mean ± S.E.M. $^{**}P < 0.01$; n.s., not significant. The control data are the same as in Fig. 6A. Data are representative of two independent experiments.

4.2. Treatment of mice with PPE and test drugs

Mice were sedated with 2% isoflurane and then administered intratracheally with PPE (15 or 20 U/kg) followed by the test compound (various doses) contained in a vehicle (0.9% NaCl; 1 ml/kg) via micropipette (P200). For control mice, the 0.9% NaCl vehicle alone was administered by the same procedure.

4.3. Preparation of BALF and cell count method

BALF was collected by cannulating the trachea and lavaging the lung with 1 ml of sterile PBS containing 50 U/ml heparin (2 times). About 1.8 ml of BALF was routinely recovered from each animal. The total cell number was counted using a hemocytometer. Cells were stained with Diff-Quik reagents after centrifugation in a Cytospin® 4 (Thermo Electron Corporation, Waltham, MA), and the ratio of number of neutrophils to total cell number was determined to calculate the number of neutrophils.

4.4. Histopathological analysis

Lung tissue samples were fixed in 10% formalin neutral buffer solution for 24 h at a pressure of 25 cmH_2O, and then embedded in paraffin before being cut into 4 μm-thick sections. Sections were stained first with Mayer's hematoxylin and then with 1% eosin alcohol solution (H & E staining). Samples were mounted with malinol and inspected with the aid of an Olympus BX51 microscope (Tokyo, Japan).

To determine the MLI, 20 lines (800 μm) were drawn randomly on the image of a section and intersection points with alveolar walls were counted to determine the MLI.[26] This morphometric analysis was conducted by an investigator blinded to the study protocol.

4.5. Measurement of airway resistance and $FEV_{0.1}/FVC$

Respiratory function and airway resistance were monitored with a computer-controlled small-animal ventilator (FlexiVent, SCIREQ, Montreal, Canada), as described previously.[19,23] Mice were anesthetized with chloral hydrate (500 mg/kg), a tracheotomy was performed, and an 8 mm section of metallic tube was inserted into the trachea. Mice were mechanically ventilated at a rate of 150 breaths/min, using a tidal volume of 8.7 ml/kg and a positive end-expiratory pressure of 2–3 cmH_2O.

For measurement of methacholine-induced increases in airway resistance, mice were exposed to nebulized methacholine (5 mg/ml) five times for 20 *sec* with a 40 *sec* interval, and airway resistance was measured after each methacholine challenge by the snapshot technique. All data were analysed using FlexiVent software.

Determination of the FEV0.1/FVC (forced expiratory volume in the first 0.1 s to forced vital capacity) ratio was performed with the same computer-controlled small-animal ventilator connected to a negative pressure reservoir (SCIREQ, Montreal, Canada), as described previously.[19,23] Mice were tracheotomised and ventilated as described above. The lung was inflated to 30 cmH_2O over one second and held at this pressure. After 0.2 *sec*, the pinch valve (connected to ventilator) was closed and after a further 0.3 *sec*, the shutter valve (connected to negative pressure reservoir) was opened for exposure of the lung to the negative pressure. The negative pressure was held for 1.5 *sec* to ensure complete expiration. The FEV0.1/FVC ratio was determined using FlexiVent software.

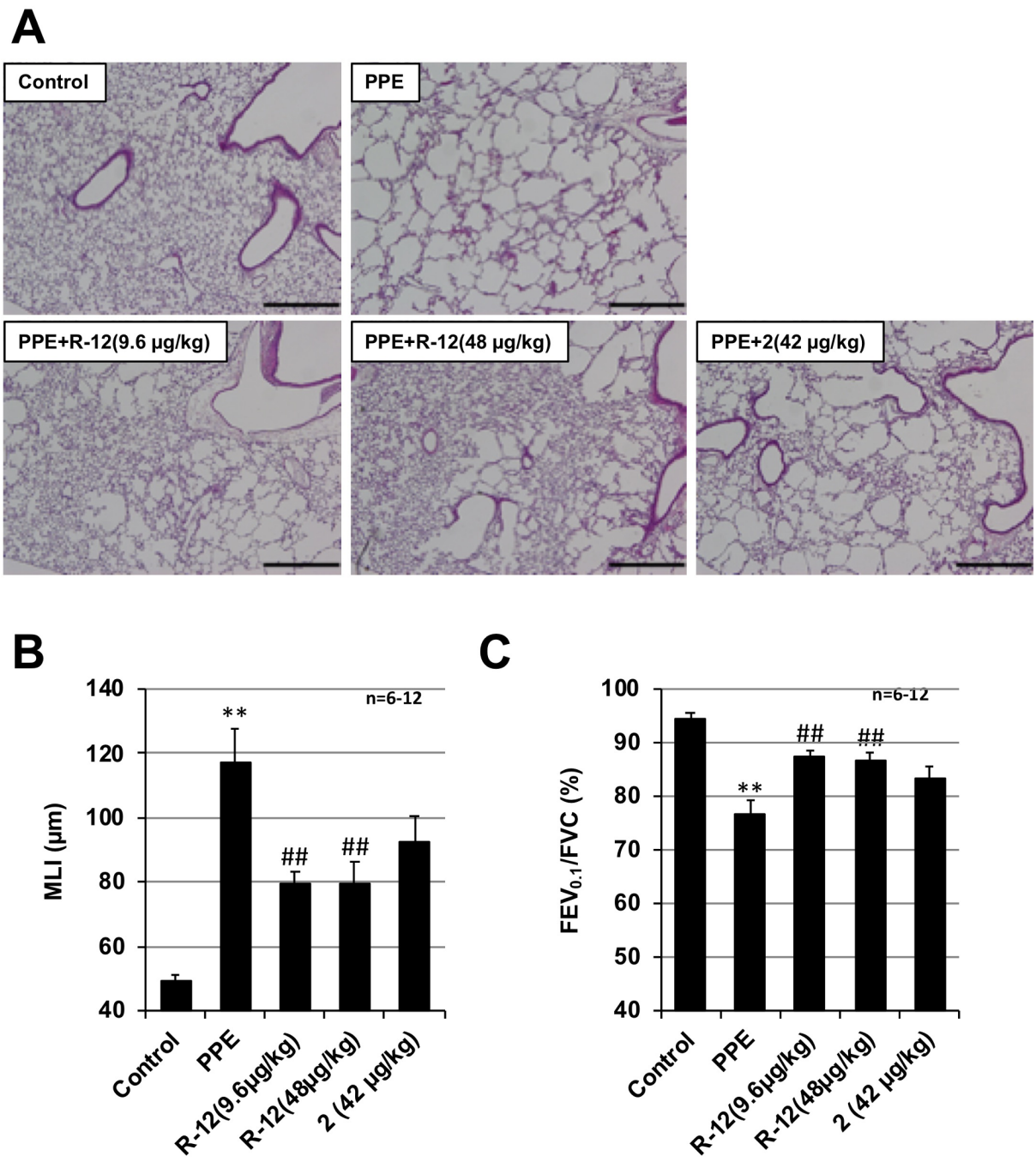

Fig. 6. Effect of **2** and (*R*)-(–)-**12** on PPE-induced pulmonary damage and dysfunction. Mice were treated with or without (control) PPE (15 U/kg) once only on day 0. The indicated doses of **2** or (*R*)-(–)-**12** were administered intratracheally once daily for 14 days (from day 0 to day 13) (A-C). Sections of pulmonary tissue were prepared on day 14 and subjected to histopathological examination (H & E staining) (scale bar, 500 μm) (A). Airspace size was estimated by determining the MLI as described in the Materials and Methods (B). $FEV_{0.1}$/FVC values were determined on day 14 as described in the Materials and Methods (C). Values represent mean ± S.E.M. $^{**}P < 0.01$ (versus control); $^{\#}P < 0.05$ (versus PPE only). Data are representative of two independent experiments.

4.6. Real-time reverse transcription polymerase chain reaction (RT-PCR) analysis.

Total RNA was extracted from lung tissue using an RNeasy kit according to the manufacturer's protocol. Samples were reverse-transcribed using the PrimeScript® kit described above. The synthesized cDNA was used in real-time PCR experiments with SsoAdvanced Universal SYBR Green Supermix and analyzed with a Bio-Rad (Hercules, CA) CFX96™ real-time system and CFX Manager™ software. Specificity was confirmed by electrophoretic analysis of reaction products and by the inclusion of template- or reverse transcriptase-free controls. To normalize the amount of total RNA present in each reaction, hypoxanthine phosphoribosyltransferase 1 (HPRT1) cDNA was used as an internal standard. Primers were designed using Primer-BLAST websites. Primers sequences will be provided upon request.

4.7. Measurement of GST activity

Left lung homogenates were prepared 24 h after (*R*)-(–)-**12** administration, GST activity in the homogenates was measured with the aid of a GST assay kit according to the manufacturer's protocol. GST activity was expressed relative to activity in the control sample.

4.8. Filter-binding assay

The filter-binding assay was performed as described previously[21] with some modifications. Membrane fractions prepared from Chinese Hamster Ovary (CHO)-K1 cells expressing human muscarinic M2 receptor (hM_2R) or human muscarinic M3 receptor (hM_3R) (Membrane Target Systems, Perkin-Elmer Life and Analytical Sciences, Boston, MA; protein concentration, 8 μg/well) were incubated with 2 nM [^{3}H]NMS (*N*-methyl-[^{3}H]-scopolamine methylchloride) (85.5 Ci/mmol) at room temperature for 2 h in 200 μL PBS in the presence of each compound. A range of concentrations (10^{-11} to 10^{-6} M) of each compound was tested in triplicate to generate competition curves. Non-specific binding was determined in the presence of atropine (2.5 μM). The samples were passed through a GF/C filter (Filtermat A, PerkinElmer Life and Analytical Sciences, Boston, MA) that was pre-incubated for 1 h with 1.0% polyethylenimine, and washed four times with ice-cold wash buffer (50 mM Tris/HCl (pH 7.4), 100 mM NaCl, 0.05% Tween-80). Filters were then dried for 30 min before attachment to MeltiLex A (melt-on scintillation sheet; PerkinElmer Life and Analytical Sciences, Boston, MA). The radioactivity remaining on the filter was monitored with a MicroBeta Trilux microplate scintillation counter (PerkinElmer Life and Analytical Sciences, Boston, MA). Affinities at equilibrium were determined as equilibrium dissociation constant (K_i) values after correcting the experimentally determined IC_{50} values with the experimentally determined NMS K_d value for hM_2R or hM_3R and the concentration of NMS, as described previously.[21] All adjustments were performed using Prism (GraphPad Software, Inc., San Diego, CA).

4.9. Statistical analysis

All values are expressed as the mean ± S.E.M. Two-way ANOVA followed by the Tukey test or Dunnett test for unpaired results was used to evaluate differences between three or more groups. Differences were considered to be significant for values of $P < 0.05$.

5. Financial disclosure

This work was supported by Grants-in-Aid for Scientific Research from the Ministry of Health, Labour, and Welfare of Japan, as well as the Japan Science and Technology Agency and Grants-in-Aid for Scientific Research from the Ministry of Education, Culture, Sports, Science and Technology, Japan. This research was also supported by the Pharmacological Research Foundation Tokyo, the Takeda Science Foundation, and the Suzuken Memorial Foundation.

6. Author contributions statement

Participated in research design: YY, KT, NY, YF, TM.
Conducted experiments: YY, KT, NY, TA, YK, AT.
Contributed new reagents or analytic tools: MK, MT, YF.
Performed data analysis: YY, KT, NY, TA, TM.
Wrote or contributed to the writing of the manuscript: YY, KT, NY, TA, YK, AT, MK, MT, YF, TM.

Declaration of Competing Interest

Tohru Mizushima is Chairman of LTT Bio-Pharma Co., Ltd. Teita Asano and Mitsuko Takenaga are employees of an endowed research division of LTT Bio-Pharma Co., Ltd.

Appendix A. Supplementary data

Supplementary data to this article can be found online at https://doi.org/10.1016/j.bmc.2019.06.016.

References

1. Rabe KF, Hurd S, Anzueto A, et al. Global strategy for the diagnosis, management, and prevention of chronic obstructive pulmonary disease: GOLD executive summary. *Am J Respir Crit Care Med.* 2007;176:532–555.
2. Vogelmeier CF, Criner GJ, Martinez FJ, et al. Global Strategy for the Diagnosis, Management, and Prevention of Chronic Obstructive Lung Disease 2017 Report. GOLD Executive Summary. *Am J Respir Crit Care Med.* 2017;195(2017):557–582.
3. Vestbo J, Hurd SS, Agusti AG, et al. Global strategy for the diagnosis, management, and prevention of chronic obstructive pulmonary disease: GOLD executive summary. *Am J Respir Crit Care Med.* 2013;187:347–365.
4. Barnes PJ, Stockley RA. COPD: current therapeutic interventions and future approaches. *Eur Respir J.* 2005;25:1084–1106.
5. Tashkin DP, Celli B, Senn S, et al. A 4-year trial of tiotropium in chronic obstructive pulmonary disease. *N Engl J Med.* 2008;359:1543–1554.
6. Calverley PM, Anderson JA, Celli B, et al. Salmeterol and fluticasone propionate and survival in chronic obstructive pulmonary disease. *N Engl J Med.* 2007;356:775–789.
7. Alsaeedi A, Sin DD, McAlister FA. The effects of inhaled corticosteroids in chronic obstructive pulmonary disease: a systematic review of randomized placebo-controlled trials. *Am J Med.* 2002;113:59–65.
8. Barnes PJ. Role of HDAC2 in the pathophysiology of COPD. *Annu Rev Physiol.* 2009;71:451–464.
9. Ito K, Ito M, Elliott WM, et al. Decreased histone deacetylase activity in chronic obstructive pulmonary disease. *N Engl J Med.* 2005;352:1967–1976.
10. Di Stefano A, Caramori G, Oates T, et al. Increased expression of nuclear factor-kappaB in bronchial biopsies from smokers and patients with COPD. *Eur Respir J.* 2002;20:556–563.
11. Rajendrasozhan S, Yang SR, Edirisinghe I, Yao H, Adenuga D, Rahman I. Deacetylases and NF-kappaB in redox regulation of cigarette smoke-induced lung inflammation: epigenetics in pathogenesis of COPD. *Antioxid Redox Signal.* 2008;10:799–811.
12. Ito K, Yamamura S, Essilfie-Quaye S, et al. Histone deacetylase 2-mediated deacetylation of the glucocorticoid receptor enables NF-kappaB suppression. *J Exp Med.* 2006;203:7–13.
13. Tanaka K, Ishihara T, Sugizaki T, et al. Mepenzolate bromide displays beneficial effects in a mouse model of chronic obstructive pulmonary disease. *Nat Commun.* 2013;4:2686.
14. Chen JY. Antispasmodic activity of JB-340 (N-methyl-3-piperidyl-diphenylglycolate methobromide) with special reference to its relative selective action on the sphincter of Oddi, colon and urinary bladder of the dog. *Arch Int Pharmacodyn Ther.* 1959;121:78–84.
15. Buckley JP, De FJ, Reif EC. The comparative antispasmodic activity of N-methyl-3-piperidyl diphenylglycolate methobromide (JB-340) and atropine sulfate. *J Am Pharm Assoc Am Pharm Assoc (Baltim).* 1957;46:592–594.
16. Long JP, Keasling HH. The comparative anticholinergic activity of a series of derivatives of 3-hydroxy piperidine. *J Am Pharm Assoc Am Pharm Assoc (Baltim).* 1954;43:616–619.
17. Tanaka K, Kurotsu S, Asano T, et al. Superiority of pulmonary administration of mepenzolate bromide over other routes as treatment for chronic obstructive pulmonary disease. *Sci Rep.* 2014;4:4510.
18. Kurotsu S, Tanaka K, Niino T, et al. Ameliorative effect of mepenzolate bromide against pulmonary fibrosis. *J Pharmac Exp Therapeutics.* 2014;350:79–88.
19. Tanaka K, Sato K, Aoshiba K, Azuma A, Mizushima T. Superiority of PC-SOD to other anti-COPD drugs for elastase-induced emphysema and alteration in lung mechanics and respiratory function in mice. *Am J Physiol Lung Cell Mol Physiol.* 2012;302:L1250–1261.
20. Tanaka KI, Yamakawa N, Yamashita Y, et al. Identification of Mepenzolate Derivatives With Long-Acting Bronchodilatory Activity. *Front Pharmacol.* 2018;9:344.
21. Yamashita Y, Tanaka K, Asano T, et al. Synthesis and biological comparison of enantiomers of mepenzolate bromide, a muscarinic receptor antagonist with bronchodilatory and anti-inflammatory activities. *Bioorg Med Chem.* 2014;22:3488–3497.
22. Olshansky B, Ebinger U, Brum J, Egermark M, Viegas A, Rekeda L. Differential pharmacological effects of antimuscarinic drugs on heart rate: a randomized, placebo-controlled, double-blind, crossover study with tolterodine and darifenacin in healthy participants > or = 50 years. *J Cardiovasc Pharmacol Ther.* 2008;13:241–251.
23. Tanaka K, Tanaka Y, Miyazaki Y, et al. Therapeutic effect of lecithinized superoxide dismutase on pulmonary emphysema. *J Pharmacol Exp Therapeutics.* 2011;338:810–818.
24. Kruse AC, Hu J, Pan AC, et al. Structure and dynamics of the M3 muscarinic acetylcholine receptor. *Nature.* 2012;482:552–556.
25. Ghorani V, Boskabady MH, Khazdair MR, Kianmeher M. Experimental animal models for COPD: a methodological review. *Tob Induc Dis.* 2017;15:25.
26. Weibel ER. Principles and methods for the morphometric study of the lung and other organs. *Lab Invest.* 1963;12:131–155.